Optik - International Journal for Light and Electron Optics 179 (2019) 89–98

Contents lists available at ScienceDirect

Optik

journal homepage: www.elsevier.com/locate/ijleo

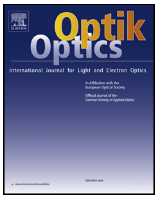

Original research article

The linear and nonlinear optical response of $CsGeX_3$ (X = Cl, Br, and I): The finite field and first-principles investigation

Qiaoqiao Zhang[a], Hahaer Mushahali[a], Haiming Duan[a,*], Ming-Hsien Lee[b], Qun Jing[a,*]

[a] School of Physical Science and Technology, Xinjiang University, 666 Shengli Road, Urumqi 830046, China
[b] Department of Physics, Tamkang University, New Taipei City 25137, Taiwan

ARTICLE INFO

Keywords:
IR NLO compounds
Finite field method
Birefringence
Born effective charges

ABSTRACT

In this paper, the linear and second order nonlinear optical properties of $CsGeX_3$ (X = Cl, Br, and I) compounds have been investigated using the finite field method combined with the density functional investigation. The obtained results are in good agreement with the experimental values. The electron density distribution nearby the fermi level is the lobe-like lone pair electrons which make the germanium-halogen polyhedron distorted. The atomic contribution to the birefringence and SHG response is analyzed using the Born effective charges, the variation of the atomic charges, and the SHG density method. The results show that the germanium and halogen atoms give main contribution to the optical anisotropic birefringence and the SHG response.

1. Introduction

Since 1960s, lots of attentions have been paid to the nonlinear optical (NLO) compounds which can be used to produce coherent light via second-harmonic generation (SHG) in solid state lasers [1]. Many NLO compounds with perfect nonlinear optical properties have been successfully synthesized, such as the very famous ultraviolet (UV) nonlinear optical crystals BBO [2], LBO family [3–6], KBBF family and KBBF-like compounds [7–24], some other acentric borates [25–40], carbonates [41–48], phosphates [49–53], and so on. Except the deep ultraviolet/ultraviolet (DUV/UV) nonlinear optical compounds, the infrared (IR) nonlinear optical compounds have also attracted plentiful attentions. Besides the commercially widely used IR NLO crystals $AgGaS_2$, $AgGaSe_2$, and $ZnGeP_2$ [54–56], lots of IR NLO compounds have also been obtained, examples including Li_3VO_4 [57,58], $Pb_{17}O_8Cl_8$ [59], $BaGa_4X_7$ (X = S, Se) [60,61], $ATeMoO_6$ [62–65], ABX_3 (A = Cs, Rb; B = Ge, Cd; X = Cl, Br, and I) [66–71], and so on [72–76]. While comparison with the DUV/UV NLO compounds, the IR NLO compounds are still relative rare, which push people to design and synthesize more IR NLO compounds to meet the needs.

To promote designing novel IR NLO compounds, lots of efforts have been made to investigate the electronic structures, the linear and nonlinear optical response. Tang et al. have investigated the linear and second-order optical response of $CsGeX_3$ (X = Cl, Br, and I) using the first principles method [77], the results show that the lattice distortion give main contribution in determining the linear and nonlinear optical responses of $CsGeX_3$ (X = Cl, Br, and I) compounds. Kang et al. have investigated the bandgap and the SHG response of the halide crystals using the first principles method [78], the results show that the $[MX_k]$ (M = center cation, X = halide anion, k = 6, 4, 3, or 2) anionic units play an important role in determining the optical response. Grant Walters et al. have investigated the electro-optic response in germanium halide perovskites using the first principles method [70].

Recently the finite field combined with first principles method have been utilized to investigate the linear and nonlinear optical

---

[*] Corresponding authors.
E-mail addresses: duan91870@sina.com (H. Duan), qunjing@xju.edu.cn (Q. Jing).

https://doi.org/10.1016/j.ijleo.2018.10.159
Received 1 September 2018; Accepted 23 October 2018

response under external electric field. Using the finite field one can get the macroscopic polarization and the linear and nonlinear optical response under different external photoelectric field, and one can also get the atomic charges and the variation of the atomic charges under external photoelectric field, which can be used to distinguish atomic contribution to the total SHG response [79–81]. This strategy has been used to investigate the microscopic origination of the SHG response in BPO_4 [82,83], KBBF family [80], $ATeMoO_6$ (A = Mg, Zn, and Cd) compounds [79], $ABCO_3F$ compounds [81], and so on.

In this paper, the finite field method combined with first principles investigation will be used to investigate the linear and nonlinear optical response of $CsGeX_3$ (X = Cl, Br, and I) compounds. The obtained refractive indices, birefringence and SHG tensors are in good agreement with the experimental values and first-principles results. The lone-pair electrons of germanium atoms are verified by the orbitals nearby the fermi level. And the atomic contribution to the optical anisotropic birefringence and the SHG response are analyzed using the Born effective charges, the variation of the atomic charges, and the SHG density method. The results show that the germanium and halogen atoms give main contribution to the birefringence and the SHG response.

2. Numerical calculations details

The macroscopic polarization under different electric field can be expressed as [79]

$$P_i^{(mac)} = \sum_j \chi_{ij}^{(1)} E_j + \sum_{jk} \chi_{ijk}^{(2)} E_j E_k \tag{1}$$

More details can be found in Ref. [79]. In this paper, the macroscopic polarization $P_i^{(mac)}$ was firstly calculated using the finite field methods implemented in ABINIT code [84–86], and then the refractive indices (and birefringence) and the nonlinear optical coefficients were obtained [79,80]. The ICSD data ($CsGeCl_3$: ICSD-62557; $CsGeBr_3$: ICSD-62558; $CsGeI_3$: ICSD-62559) were used to do the finite field calculations. During the calculations, the PBE-GGA functional were used, and the norm-conserving pseudopotentials(NCP) [87] were adopted. The energy cutoff was set as 40.0 hartree along with a dense k-point sample (12 × 12 × 12). For comparison, the SHG response were also calculated using the Density-Functional Perturbation Theory (DFPT) method [88] implemented in ABINIT code. During the calculation, the LDA functional was used, and same values about energy cutoff and k-point sample like finite field calculations were used.

The electronic structure, the Born effective charges and optical properties of $CsGeX_3$ (X = Cl, Br, I) were also evaluated using the CASTEP code [89]. During the calculation, the GGA-PBE functional [90], and the NCP-type pseudopotentials [91,92] were adopted. The kinetic energy cutoffs were set as 830 eV for $CsGeCl_3$, and 440 eV for $CsGeBr_3$ and $CsGeI_3$ compounds. The k-point meshes were set as 6 × 6×6 for these compounds. The refractive indices, the birefringence, and the nonlinear optical coefficients are obtained using the method described in Ref. [93], Ref. [94], and Ref. [101].

3. Results and discussions

3.1. The electronic structures and the lone pair electrons

Using the method described above, the band structures, the projected density of states (PDOS), and the electron structures of $CsGeX_3$ (X = Cl, Br, and I) were obtained. The obtained band structures of $CsGeX_3$ (X = Cl, Br, and I) are shown in Fig. 1. As shown in Fig. 1, all of these compounds are direct bandgap compounds whose maximum valence band and minimum conduction band are all located at the Z point. The obtained bandgaps of $CsGeX_3$ (X = Cl, Br, and I) compounds are 1.95, 1.27, and 0.80 eV, respectively. The obtained bandgaps are all smaller than that of experimental values. The underestimation of the bandgaps may have relation with the derivative discontinuity of the exchange-correlation energy [1,95,96].

The obtained projected densities of states (PDOS) are also shown in Fig. 1. As shown in Fig. 1, these compounds own similar projected densities of states. Take $CsGeCl_3$ for example. For $CsGeCl_3$ compound, the localized Cs-p states are found nearby -8.2 eV, indicating its ionic characters. The hybrid Ge sp – Cl p states are found at the top of the valence band (from −8.5 eV to the Fermi level), indicating the covalent interaction between germanium and halogen atoms. The hybrid states from the cesium, germanium and halogen atoms are also found at the bottom of the conduction bands. It is well known that the optical properties have relation with the electron transition among the states at the top of the valence band and the bottom of the conduction band [40,50,58,97–103], hence one can deduce that polyhedron containing germanium and halogen atoms would give main contribution to the linear and nonlinear optical properties of $CsGeX_3$ (X = Cl, Br, and I) compounds.

It is interesting to note that, for the $CsGeCl_3$ compound, the hybrid Ge s-Cl p states are found at the energy region (-8.5, -7) eV which is the bonding stats of Ge-Cl chemical bond, and the hybrid Ge sp – Cl p states are found at the energy region (-5, 0) eV which is coming from the interaction between the antibonding states of Ge s-Cl p and the Ge p states. Similar hybrid states from the germanium and halogen atoms can also be found in other $CsGeX_3$ (X = Br, I) compounds (shown in Fig. 1). According to the revised model about the formation of the lone-pair electrons in post transition-metal atoms [104–106], the authors believe that the germanium sp – halogen p states nearby the Fermi level would own the electron density distribution like lone-pair electrons. The states nearby the Fermi level are shown in Fig. 2. It clearly shows the lobe-like lone pair electrons. The lone pair electrons around the germanium make the germanium-halogen polyhedron distorted, which would play an important role in determining the linear and nonlinear optical response under the external photoelectric field. The distorted germanium-halogen polyhedrons are further shown in Fig. S1 in supporting information (SI).

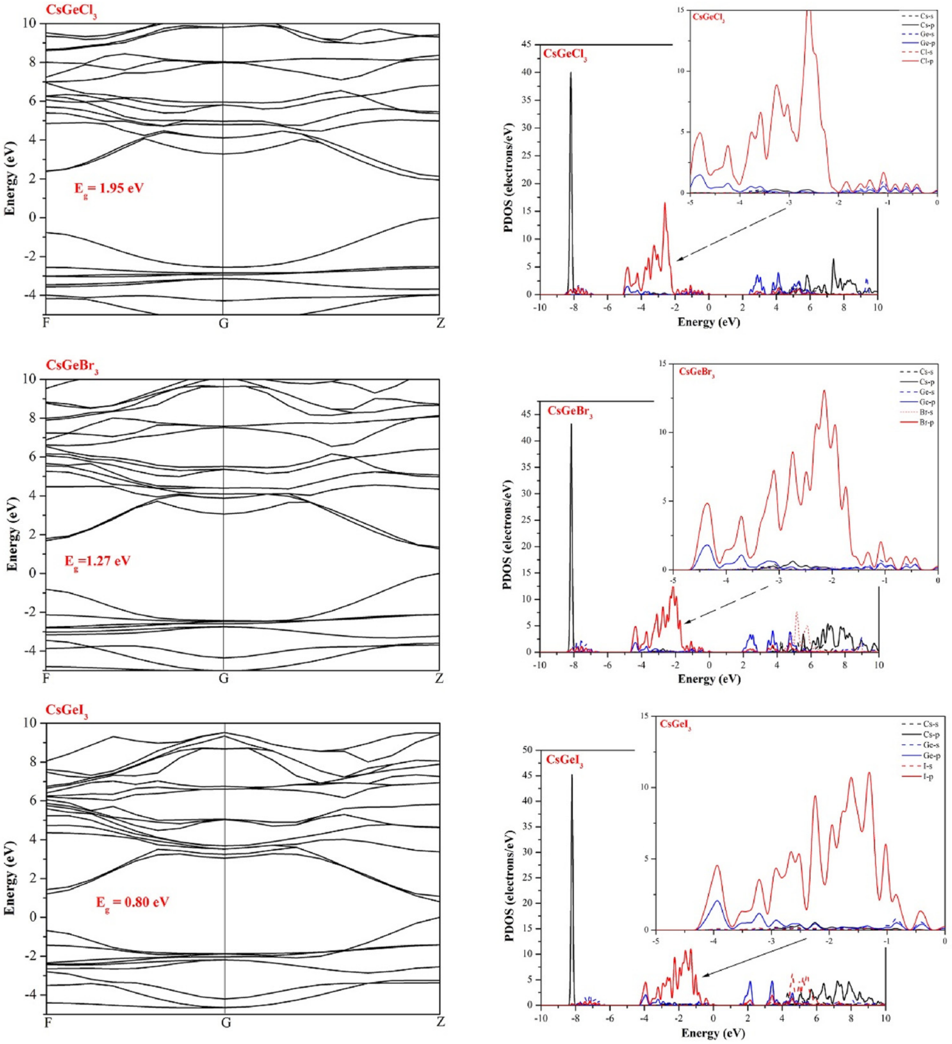

Fig. 1. The obtained band structures and the projected density of states (PDOS) of CsGeX$_3$ (X = Cl, Br, and I) compounds using the DFT method.

3.2. The refractive indices, birefringence and the Born effective charges

Using the method described above, the macroscopic polarization under different external electric field was obtained. The refractive indices along different optical principle axis can be obtained using the equation about the first order linear optical term of the macroscopic polarization ($P_i^{(1)} = \sum_j \chi_{ij} E_j$) and ($n_i = \sqrt{1 + 4\pi\chi_{ii}}$) [79,80]. The obtained refractive indices and the birefringence are shown in Table 1. For comparison, the refractive indices and birefringence of CsGeX$_3$ (X = Cl, Br, and I) are also obtained using density functional theory implemented in the CASTEP code. As shown in Table 1 and Fig. 3, the refractive indices and birefringence obtained from the finite-field methods implemented in ABINIT code [84–86] are similar with the one obtained using the CASTEP code [89]. One can also find out that although the birefringence of these CsGeX$_3$ (X = Cl, Br, and I) compounds are relative small, but they own relative small refractive indices dispersion which would make these compounds meet the phase-matching conditions. Actually these compounds are all phase matchable [66,67].

To better understand the atomic contribution to the refractive indices and the birefringence, the Born effective charges have also been calculated. More details about the Born effective charges can be found in Ref. [1], and Ref. [107]. The obtained Born effective charges are listed in Table 2 and Table S1 in SI. For CsGeX$_3$ (X = Cl, Br, and I) compounds crystallized into the $3m$ point group, the polarization of the ordinary light is in the xy plane, and the polarization of the extraordinary light is in the z axis. As shown in Table 2, for the alkali metal atoms, the Born effective charges in xy plane are similar with the Born effective charges along Z axis. The difference of the Born effective charges along the direction of n_o and n_e ($\Delta q^{(\mathrm{Born})}$) is very small (from 0.008 to 0.03 for CsGeX$_3$ compounds), implying the alkali metal atoms give relative small contribution to the birefringence. For the germanium and halogen atoms, as shown in Table 2 and Table S1 in SI, the Born effective charges in xy plane are larger than the Born effective charges along the z axis, indicating these atoms give positive contribution to the birefringence. The positive contribution from the germanium and

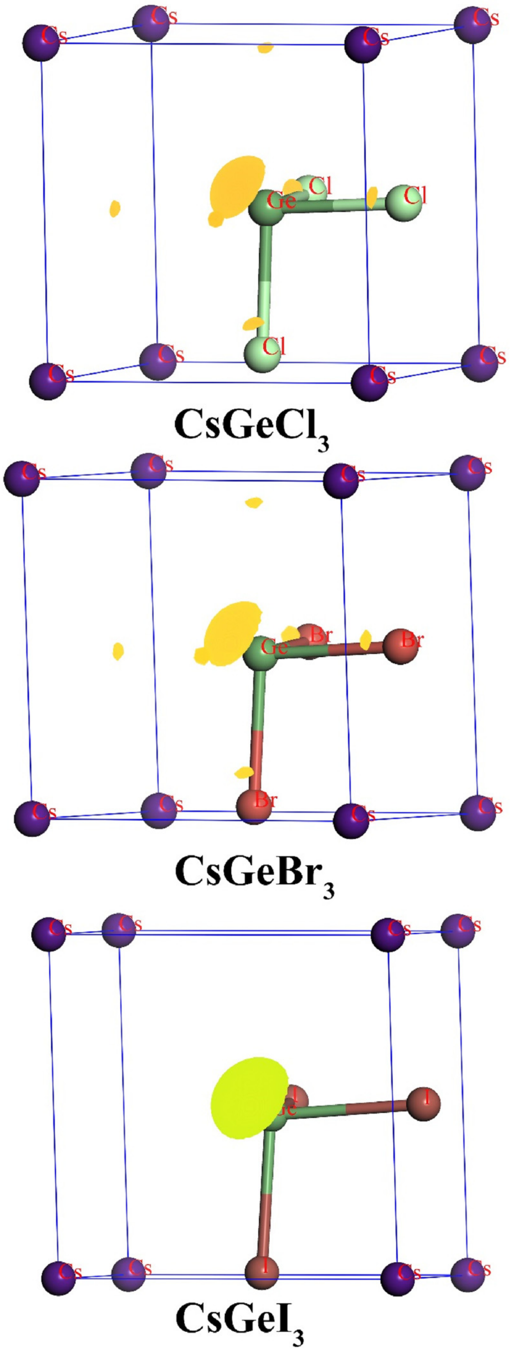

Fig. 2. The lobe-like electron density found in the orbitals nearby the fermi level of $CsGeX_3$ (X = Cl, Br, and I) compounds.

halogen atoms may have relation with the covalent interaction between the germanium and halogen atoms, and the distorted polyhedron induced by the lone pair electrons around the germanium atoms.

3.3. The SHG response and the atomic contributions

For the $CsGeX_3$ (X = Cl, Br, and I) compounds crystallized in *3 m* point group, there are three different independent nonzero SHG tensors: d_{15}, d_{22}, and d_{33}. Hence the second term of the macroscopic polarization can be expressed as:

$$P_1^{(2)} = 2\chi_{15}E_3E_1 - 2\chi_{22}E_1E_2 \quad (2)$$

Table 1
The obtained refractive indices, birefringence and nonlinear optical coefficients using different methods.

		$CsGeCl_3$	$CsGeBr_3$	$CsGeI_3$
finite field	n_o	1.927	2.219	2.575
	n_e	1.884	2.193	2.549
	Δn	0.043	0.026	0.026
DFT	n_o	1.912	2.174	2.545
	n_e	1.867	2.133	2.516
	Δn	0.045	0.040	0.029
finite field	d_{15}	3.569	15.506	67.735
	d_{22}	−0.412	−7.917	−46.865
	d_{33}	8.502	20.968	31.548
DFPT	d_{15}	5.391	21.313	177.244
	d_{22}	1.468	13.080	110.600
	d_{33}	10.633	25.295	5.558

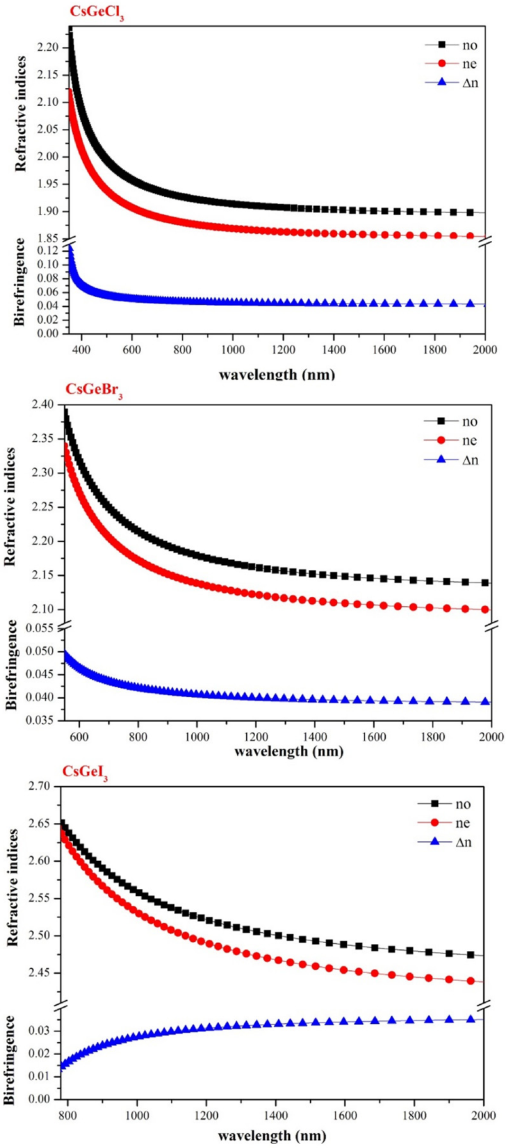

Fig. 3. The obtained refractive indices and birefringence using the DFT methods.

Table 2
The obtained diagonal tensor of atomic Born effective charges of $CsGeX_3$ (X = Cl, Br, and I) compounds. More details about the Born effective charges of $CsGeX_3$ (X = Cl, Br, and I) can be found in Table S1 in SI.

Compounds	Atoms	q_{xx}	q_{yy}	q_{zz}	$\Delta q^{(Born)}$
CsGeCl3	Cs	1.12383	1.12383	1.11552	0.00831
	Ge	3.05867	3.05867	2.69519	0.36348
	Cl1	−0.94109	−1.84724	−1.27024	0.32915
	Cl2	−1.62070	−1.16763	−1.27024	0.10261
	Cl3	−1.62070	−1.16763	−1.27024	0.10261
CsGeBr3	Cs	1.13943	1.13943	1.11047	0.02896
	Ge	3.36581	3.36581	2.90198	0.46383
	Br1	−0.90513	−2.09837	−1.33748	0.43235
	Br2	−1.80006	−1.20344	−1.33748	0.13404
	Br3	−1.80006	−1.20344	−1.33748	0.13404
CsGeI3	Cs	1.12719	1.12719	1.09251	0.03468
	Ge	3.80943	3.80943	3.12286	0.68657
	I1	−0.94299	−2.34809	−1.40513	0.46214
	I2	−1.99682	−1.29427	−1.40513	0.11086
	I3	−1.99682	−1.29427	−1.40513	0.11086

$$P_2^{(2)} = -\chi_{22}E_1^2 + \chi_{22}E_2^2 + 2\chi_{15}E_2E_3 \tag{3}$$

$$P_3^{(2)} = \chi_{15}E_1^2 + \chi_{15}E_2^2 + \chi_{33}E_3^2 \tag{4}$$

In which the $P_1^{(2)}$, $P_2^{(2)}$, and $P_3^{(2)}$ are the macroscopic polarization along x, y, and z axes, and the E_1, E_2, and E_3 are the external electric field along x, y, and z axes, the $\chi_{15} = 2d_{15}$, $\chi_{22} = 2d_{22}$, and $\chi_{33} = 2d_{33}$ are the SHG coefficients tensors. The obtained SHG tensors are also shown in Table 1. For comparison, the SHG tensors are also obtained using the DFPT methods. As shown in Table 1, the obtained SHG are in excellent agreement with the first principles results.

In order to analyze the atomic contribution to the second order nonlinear optical coefficients, the atomic charges and the variation of the atomic charge (ΔQ) were calculated using the finite-field method. The variation of the atomic charge ΔQ are the difference of the atomic charges when the external electric field was changed as 0.00001 atomic unit (a.u.). The obtained ΔQ values are shown in Table 3. As shown in Table 3, for these $CsGeX_3$ (X = Cl, Br, and I) compounds, the alkali metal atoms own the smallest ΔQ values, which indicates these atoms give very little contribution to the total nonlinear optical response, while the germanium atoms and the halogen atoms own relative large ΔQ values (especially for the halogen atoms) which indicates these atoms give main contribution to the nonlinear optical response under the external electric field.

To further investigate the atomic contribution to the nonlinear optical response, a SHG-density technique are adopted. The SHG-density method was used to visualize the states relevant to the SHG in real space [108]. It was performed by using the effective SHG of each band as weighting coefficient to sum the probability densities of all occupied or unoccupied states [108]. More details about the SHG-density method can be seen in Ref. [108]. The total SHG coefficients are divided into the contribution of virtual-electron, and virtual-hole processes. The SHG-density method can give the atomic contribution from the virtual-electron occupied (marked as veocc), the virtual-electron unoccupied (marked as veunocc), the virtual-hole occupied (marked as vhocc) and the virtual-hole unoccupied (marked as vhunocc) processes. Generally speaking the veocc and vhunocc process give main contribution to the total SHG response, hence herein the authors would just show the SHG density from the veocc and vhunocc process. The obtained SHG density of $CsGeX_3$ (X = Cl, Br, and I) compounds are shown in Fig. 4 (for $CsGeCl_3$) and Figure S2 (for $CsGeBr_3$) and Figure S3 (for $CsGeI_3$) in SI. In Figs. 4, S2 and S3, the color part represents the SHG density from the veocc process, and the white-black part represents the SHG density from the vhunocc process. As shown in Figs. 4, S2, and S3, the SHG density are mainly on the germanium and halogen atoms, indicating the germanium and halogen atoms give main contribution to the total SHG response.

4. Conclusions

In this paper, the linear and second order nonlinear optical properties of $CsGeX_3$ (X = Cl, Br, and I) compounds have been investigated using the finite field method combined with the density functional investigation. The obtained results are in good agreement with the experimental values. The electron density distribution nearby the fermi level is the lobe-like lone pair electrons which make the germanium-halogen polyhedron distorted. The Born effective charges analysis shows that the cesium give little

Table 3
The obtained variation of atomic charges (ΔQ, $\times 10^{-5}$) of $CsGeX_3$ (X = Cl, Br, and I) under external electric field [111].

	Cs	Ge	X1	X2	X3
$CsGeCl_3$	0.002	0.782	0.705	3.074	0.307
$CsGeBr_3$	0.003	1.276	0.817	3.185	0.255
$CsGeI_3$	0.004	1.782	0.722	2.498	0.140

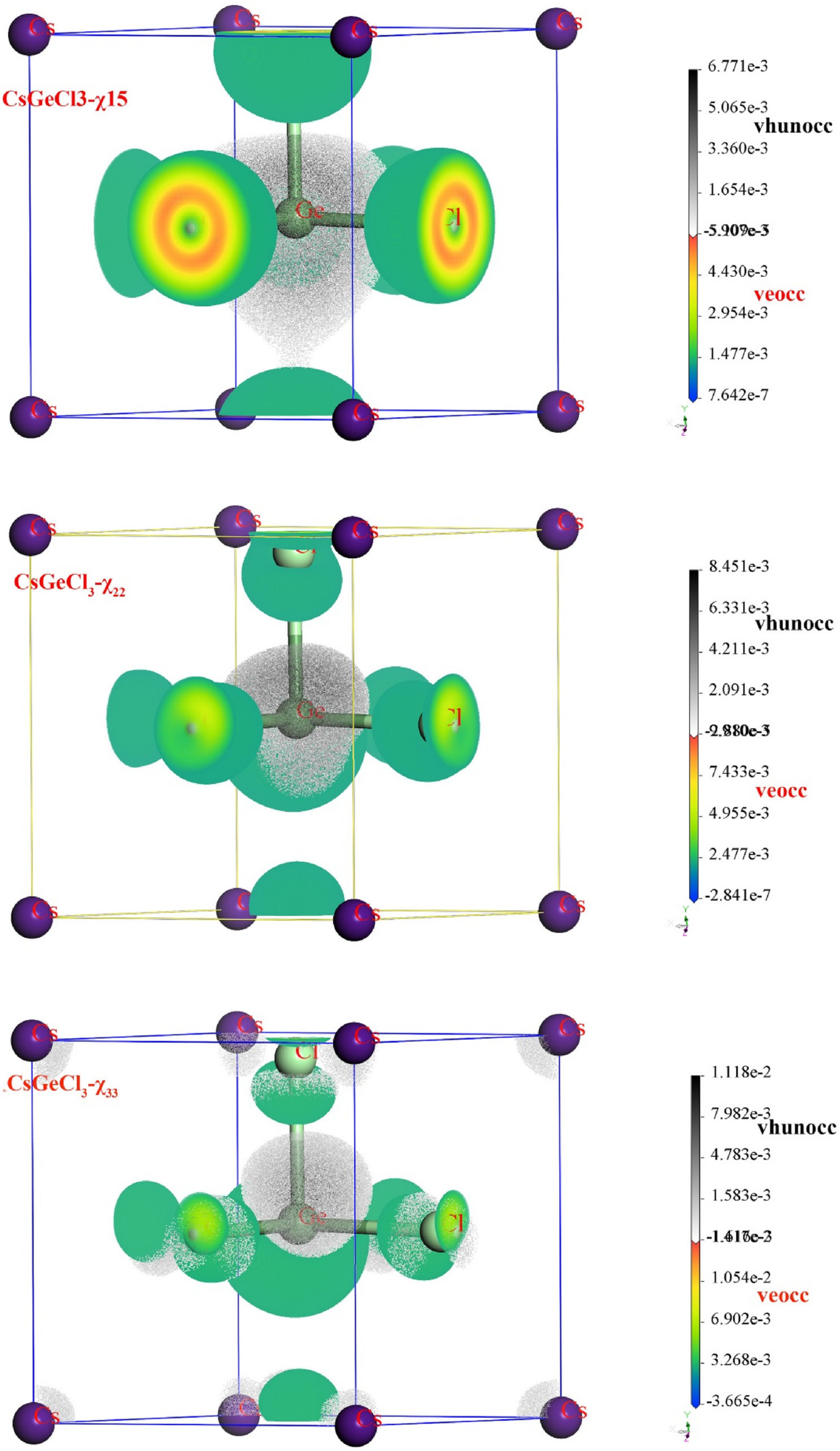

Fig. 4. The obtained SHG density of $CsGeCl_3$ compounds.

contribution to the optical anisotropic birefringence, and the germanium and halogen atoms give main contribution to the total birefringence. The analysis using the variation of atomic charges and the SHG density methods shows that the germanium and halogen atoms give main contribution to the SHG response.

Acknowledgements

This work is supported by the National Natural Science Foundation of China (Grant Nos. 11864040, 11664038), the Natural Science Foundation of Xinjiang Uygur Autonomous Region of China (Grant No. 2018D01C072), the Science and Technology Research Program for Colleges and Universities in the Department of Education in Xinjiang Uygur Autonomous Region of China (Grant No. XJEDU2017M006).

Appendix A. Supplementary data

Supplementary material related to this article can be found, in the online version, at doi:https://doi.org/10.1016/j.ijleo.2018.10.159.

References

[1] Q. Jing, G. Yang, J. Hou, M. Sun, H. Cao, Positive and negative contribution to Birefringence in a family of carbonates: a born effective charges analysis, J. Solid State Chem. 244 (2016) 69–74.
[2] C. Chen, B. Wu, A. Jiang, G. You, A new-type ultraviolet SHG crystal - Beta-BaB_2O_4, Sci. Sin., Ser. B, Chem. Biol. Agric. Med. Earth Sci. 28 (1985) 235–243.
[3] C. Chen, Y. Wu, A. Jiang, B. Wu, G. You, R. Li, S. Lin, New nonlinear optical crystal - LiB_3O_5, J. Opt. Soc. Am. B 6 (1989) 616–621.
[4] Y.C. Wu, T. Sasaki, S. Nakai, A. Yokotani, H.G. Tang, C.T. Chen, CsB_3O_5 - a new nonlinear optical crystal, Appl. Phys. Lett. 62 (1993) 2614–2615.
[5] Y. Mori, S. Nakajima, A. Miyamoto, M. Inagaki, T. Sasaki, Generation of ultraviolet light by using new nonlinear optical crystal $CsLiB_6O_{10}$, 1st Annual International Conference on Solid State Lasers for Application to Inertial Confinement Fusion, Proceedings 2633 (1995) 299–307.
[6] J.M. Tu, D.A. Keszler, $CsLiB_6O_{10}$ - a noncentrosymmetric polyborate, Mater. Res. Bull. 30 (1995) 209–215.
[7] C. Chen, Z. Xu, D. Deng, J. Zhang, G.K.L. Wong, B. Wu, N. Ye, D. Tang, The vacuum ultraviolet phase-matching characteristics of nonlinear optical $KBe_2BO_3F_2$ crystal, Appl. Phys. Lett. 68 (1996) 2930.
[8] McMillen, C.; Kolis, J.; Liu, C.; Kaminski, A.; Ballato, J., Hydrothermal Growth and Properties of KBe2BO3F2 (KBBF) and RbBe2BO3F2 (RBBF) Single Crystals. Advanced Photonics & Renewable Energy, OSA Technical Digest (CD) (Optical Society of America, 2010), paper NThC6.
[9] H. Wu, H. Yu, S. Pan, P.S. Halasyamani, Deep ultraviolet nonlinear optical material $K_3Sr_3Li_2Al_4B_6O_{20}F$: addressing the structural instability problem in $KBe_2BO_3F_2$, Inorg. Chem. 56 (2017) 8755–8758.
[10] G. Peng, et al., $NH_4Be_2BO_3F_2$and Gamma-Be_2BO_3F: Overcoming the Layering Habit in $KBe_2BO_3F_2$ for the Next Generation Deep-Ultraviolet Nonlinear Optical Materials, Angew. Chem. Int. Ed. Engl. 57 (2018) 8968–8972.
[11] G. Yang, K. Wu, Two-dimensional deep-ultraviolet beryllium-free $KBe_2BO_3F_2$ family nonlinear optical monolayer, Inorg. Chem. 57 (2018) 7503–7506.
[12] H. Yu, N.Z. Koocher, J.M. Rondinelli, P.S. Halasyamani, Pb_2BO_3I: A Borate Iodide with the Largest Second-Harmonic Generation (SHG) Response in the $KBe_2BO_3F_2$ (KBBF) Family of Nonlinear Optical (NLO) Materials, Angew. Chem. Int. Ed. Engl. 57 (2018) 6100–6103.
[13] H. Wu, G. Wang, X.Y. Wang, X. Zhang, Y. Zhu, C.T. Chen, Sellmeier equations and phase-matching characteristics of the nonlinear optical crystal $RbBe_2BO_3F_2$, Appl. Opt. 48 (2009) 4118–4123.
[14] L. Liu, H. Zhou, X. He, X. Zhang, X. Wang, F. Lu, C. Zhang, W. Zhou, C. Chen, Hydrothermal growth and optical properties of $RbBe_2BO_3F_2$ crystals, J. Cryst. Growth 348 (2012) 60–64.
[15] L.-R. Wang, G.-L. Wang, X. Zhang, L.-J. Liu, X.-Y. Wang, Y. Zhu, C.-T. Chen, Generation of ultraviolet radiation at 266 nm with $RbBe_2BO_3F_2$ crystal, Chin. Phys. Lett. (2012) 29.
[16] N. Zhai, L. Wang, L. Liu, X. Wang, Y. Zhu, C. Chen, Measurement of thermal refractive index coefficients of nonlinear optical crystal $RbBe_2BO_3F_2$, Opt. Mater. (Amst) 36 (2013) 333–336.
[17] H. Huang, C. Chen, X. Wang, Y. Zhu, G. Wang, X. Zhang, L. Wang, J. Yao, Ultraviolet nonlinear optical crystal: $CsBe_2BO_3F_2$, J. Opt. Soc. Am. B 28 (2011) 2186.
[18] H. Yu, H. Wu, S. Pan, Z. Yang, X. Hou, X. Su, Q. Jing, K.R. Poeppelmeier, J.M. Rondinelli, $Cs_3Zn_6B_9O_{21}$: A Chemically Benign Member of the KBBF Family Exhibiting the Largest Second Harmonic Generation Response, J. Am. Chem. Soc. 136 (2014) 1264–1267.
[19] Q. Huang, L. Liu, X. Wang, R. Li, C. Chen, Beryllium-free KBBF family of nonlinear optical crystals: $AZn_2BO_3X_2$ (A = Na, K, Rb; X = Cl, Br), Inorg. Chem. 55 (2016) 12496–12499.
[20] G. Yang, P. Gong, Z. Lin, N. Ye, $AZn_2BO_3X_2$ (A = K, Rb, NH_4; X = Cl, Br): new members of KBBF family exhibiting large SHG response and the enhancement of layer interaction by modified structures, Chem. Mater. 28 (2016) 9122–9131.
[21] Z. Fang, F. Liang, M. Xia, L. Liu, Q. Huang, S. Guo, X. Wang, Z. Lin, C. Chen, Two KBBF-Type beryllium borates $MBe_2B_2O_6$ (M = Sr, Ba) with a three-dimensional $(Be_2B_2O_6)\infty$ network, Inorg. Chem. 56 (2017) 12090–12093.
[22] Y. Shen, S. Zhao, Y. Yang, L. Cao, Z. Wang, B. Zhao, Z. Sun, Z. Lin, J. Luo, A new KBBF-Family nonlinear optical material with strong interlayer bonding, Cryst. Growth Des. 17 (2017) 4422–4427.
[23] M. Luo, Y. Song, F. Liang, N. Ye, Z. Lin, Pb_2BO_3Br: A Novel Nonlinear Optical Lead Borate Bromine with a KBBF-Type Structure Exhibiting Strong Nonlinear Optical Response, Inorg. Chem. Front. 5 (2018) 916–921.
[24] G.Y. Yang, K.C. Wu, Designing two-dimensional KBBF family second-harmonic generation monolayers, J. Phys. Chem. C 122 (2018) 7992–7996.
[25] F. Liang, L. Kang, P. Gong, Z. Lin, Y. Wu, Rational design of deep ultraviolet nonlinear optical materials in fluorooxoborates: toward optimal planar configuration, Chem. Mater. 29 (2017) 7098–7102.
[26] B. Zhang, G. Shi, Z. Yang, F. Zhang, S. Pan, Fluorooxoborates: beryllium-free deep ultraviolet nonlinear optical materials without layered growth, Angew. Chemie Int. Ed. 56 (2017) 3916–3919.
[27] S. Han, Y. Wang, B. Zhang, Z. Yang, S. Pan, A member of fluorooxoborates: $Li_2Na_{0.9}K_{0.1}B_5O_8F_2$ with the fundamental building block $B_5O_{10}F_2$ and a short cutoff edge, Inorg. Chem. (2018).
[28] M. Luo, L. Fei, Y. Song, D. Zhao, F. Xu, N. Ye, Z. Lin, Correction to " $M_2B_{10}O_{14}F_6$ (M = Ca, Sr): two noncentrosymmetric alkaline earth fluorooxoborates as promising next-generation deep ultraviolet nonlinear optical materials ", J. Am. Chem. Soc. 140 (2018) 6509.
[29] M. Luo, F. Liang, Y. Song, D. Zhao, F. Xu, N. Ye, Z. Lin, $M_2B_{10}O_{14}F_6$ (M = Ca, Sr): two noncentrosymmetric alkaline earth fluorooxoborates as promising next-generation deep ultraviolet nonlinear optical materials, J. Am. Chem. Soc. 140 (2018) 3884–3887.
[30] M. Luo, F. Liang, Y. Song, D. Zhao, N. Ye, Z. Lin, Rational design of the first Lead/Tin fluorooxoborates $MB_2O_3F_2$ (M = Pb, Sn), containing flexible two dimensional $[B_6O_{12}F_6]$Infinity single layers with widely divergent second harmonic generation effects, J. Am. Chem. Soc. 140 (2018) 6814–6817.
[31] Y. Wang, B. Zhang, Z. Yang, S. Pan, Cation tuned synthesis of fluorooxoborates: towards optimal deep ultraviolet nonlinear optical materials, Angew. Chem. Int. Ed. Engl. 57 (2018) 2150–2154.
[32] G.Q. Shi, Y. Wang, F.F. Zhan, B.B. Zhang, R.H. Yang, X.L. Hou, S.L. Pan, K.R. Poeppelmeier, Finding the next deep ultraviolet nonlinear optical material:

$NH_4B_4O_6F$, J. Am. Chem. Soc. 139 (2017) 10645–10648.

[33] X. Wang, Y. Wang, B. Zhang, F. Zhang, Z. Yang, S. Pan, CsB_4O_6F: a congruent-melting deep ultraviolet nonlinear optical material by combining superior functional units, Angew. Chem. Int. Ed. Engl. 56 (2017) 14119–14123.

[34] H. Wu, S. Pan, K.R. Poeppelmeier, H. Li, D. Jia, Z. Chen, X. Fan, Y. Yang, J.M. Rondinelli, H. Luo, $K_3B_6O_{10}Cl$: A New Structure Analogous to Perovskite with a Large Second Harmonic Generation Response and Deep UV Absorption Edge, J. Am. Chem. Soc. 133 (2011) 7786–7790.

[35] H. Wu, H. Yu, Z. Yang, X. Hou, X. Su, S. Pan, K.R. Poeppelmeier, J.M. Rondinelli, Designing a deep ultraviolet nonlinear optical material with a large second harmonic generation response, J. Am. Chem. Soc. 135 (2013) 4215–4218.

[36] H.W. Yu, H.P. Wu, S.L. Pan, Z.H. Yang, X. Su, F.F. Zhang, A novel deep UV nonlinear optical crystal $Ba_3B_6O_{11}F_2$, with a new fundamental building block, B_6O_{14} group, J. Mater. Chem. 22 (2012) 9665–9670.

[37] Y.Z. Huang, L.M. Wu, X.T. Wu, L.H. Li, L. Chen, Y.F. Zhang, $Pb_2B_5O_9I$: An Iodide Borate with Strong Second Harmonic Generation, J. Am. Chem. Soc. 132 (2010) 12788–12789.

[38] Z. Chen, S. Pan, Z. Yang, X. Dong, X. Su, Y. Yang, $Pb_2B_5O_9Cl$: A Chloride Borate with Second Harmonic Generation Effect, J. Mater. Sci. 48 (2012) 2590–2596.

[39] X. Dong, Q. Jing, Y. Shi, Z. Yang, S. Pan, K.R. Poeppelmeier, J. Young, J.M. Rondinelli, $Pb_2Ba_3(BO_3)_3Cl$: A Material with Large SHG Enhancement Activated by Pb-Chelated BO3 Groups, J. Am. Chem. Soc. 137 (2015) 9417–9422.

[40] Q. Jing, X. Dong, Z. Yang, S. Pan, Synthesis and optical properties of the first lead borate bromide with isolated BO_3 groups: $Pb_2Ba_3(BO_3)_3Br$, Dalton Trans. 44 (2015) 16818–16823.

[41] G. Zou, N. Ye, L. Huang, X. Lin, Alkaline-Alkaline earth fluoride carbonate crystals $ABCO_3F$ (A = K, Rb, Cs; B = Ca, Sr, Ba) as nonlinear optical materials, J. Am. Chem. Soc. 133 (2011) 20001–20007.

[42] G. Zou, L. Huang, N. Ye, C. Lin, W. Cheng, H. Huang, $CsPbCO_3F$: a strong second-harmonic generation material derived from enhancement via $P-\pi$ interaction, J. Am. Chem. Soc. 135 (2013) 18560–18566.

[43] Y. Lin, C.L. Hu, J.G. Mao, $K_2Pb_3(CO_3)_3F_2$ and $KCdCO_3F$: novel fluoride carbonates with layered and 3D framework structures, Inorg. Chem. 54 (2015) 10407–10414.

[44] T.T. Tran, J. He, J.M. Rondinelli, P.S. Halasyamani, $RbMgCO_3F$: a new beryllium-free deep-ultraviolet nonlinear optical material, J. Am. Chem. Soc. 137 (2015) 10504–10507.

[45] G. Zou, G. Nam, H.G. Kim, H. Jo, T.-S. You, K.M. Ok, $ACdCO_3F$ (A = K and Rb): New Noncentrosymmetric Materials with Remarkably Strong Second-Harmonic Generation (SHG) Responses Enhanced Via π Interaction, RSC Adv. 5 (2015) 84754–84761.

[46] Q. Li, G. Zou, C. Lin, N. Ye, Synthesis and characterization of $CsSrCO_3F$ – a beryllium-free new deep-ultraviolet nonlinear optical material, New J. Chem. 40 (2016) 2243–2248.

[47] L. Huang, Q. Wang, C. Lin, G. Zou, D. Gao, J. Bi, N. Ye, Synthesis and characterization of a new beryllium-free deep-ultraviolet nonlinear optical material: $Na_2GdCO_3F_3$, J. Alloys. Compd. 724 (2017) 1057–1063.

[48] W. Zhang, P.S. Halasyamani, Crystal growth and optical properties of a UV nonlinear optical material $KSrCO_3F$, CrystEngComm 19 (2017) 4742–4748.

[49] P. Yu, L.M. Wu, L.J. Zhou, L. Chen, Deep-ultraviolet nonlinear optical crystals: $Ba_3P_3O_{10}X$ (X = Cl, Br), J. Am. Chem. Soc. 136 (2014) 480–487.

[50] Z. Chen, Y. Fang, W. Zhang, W. Chen, X. Lu, Q. Jing, M.H. Lee, $ALiZnP_2O_7$(A = Rb, Cs): Two Mixed Alkali Zinc Pyrophosphates Featuring a $[Li_2Zn_2P_4O_{20}]^{14-}$ Anionic Skeleton, Inorg. Chem. (2018), https://doi.org/10.1021/acs.inorgchem.8b01140.

[51] L. Li, Y. Wang, B.H. Lei, S. Han, Z. Yang, K.R. Poeppelmeier, S. Pan, A new deep-ultraviolet transparent orthophosphate $LiCs_2PO_4$ with large second harmonic generation response, J. Am. Chem. Soc. 138 (2016) 9101–9104.

[52] S. Zhao, P. Gong, S. Luo, L. Bai, Z. Lin, Y. Tang, Y. Zhou, M. Hong, J. Luo, Tailored synthesis of a nonlinear optical phosphate with a short absorption edge, Angew. Chem. Int. Ed. Engl. 54 (2015) 4217–4221.

[53] S. Zhao, P. Gong, S. Luo, L. Bai, Z. Lin, C. Ji, T. Chen, M. Hong, J. Luo, Deep-Ultraviolet Transparent Phosphates $RbBa_2(PO_3)_5$ and $Rb_2Ba_3(P_2O_7)_2$ Show Nonlinear Optical Activity from Condensation of $[PO_4]^{3-}$ Units, J. Am. Chem. Soc. 136 (2014) 8560–8563.

[54] G.D. Boyd, H. Kasper, J.H. Mcfee, Linear and nonlinear optical properties of $AgGaS_2$, $CuGaS_2$, and $CuInS_2$, and theory of wedge technique for measurement of nonlinear coefficients, IEEE J. Quantum Electron. (1971) Qe 7, 563-&.

[55] B. Tell, H.M. Kasper, Optical and electrical properties of $AgGaS_2$ and $AgGaSe_2$, Phys. Rev. B 4 (1971) 4455–4459.

[56] G.D. Boyd, Linear and nonlinear optical properties of $ZnGeP_2$ and CdSe, Appl. Phys. Lett. 18 (1971) 301.

[57] S. Sakata, Y. Nagoshi, H. Nii, N. Ueda, H. Kawazoe, Electronic structure of second harmonic generation crystal Li_3VO_4, J. Appl. Phys. 80 (1996) 3668.

[58] Z. Chen, Z. Zhang, X. Dong, Y. Shi, Y. Liu, Q. Jing, Li_3VO_4: A Promising Mid-Infrared Nonlinear Optical Material with Large Laser Damage Threshold, Cryst. Growth Des. 17 (2017) 2792–2800.

[59] H. Zhang, M. Zhang, S. Pan, X. Dong, Z. Yang, X. Hou, Z. Wang, K.B. Chang, K.R. Poeppelmeier, $Pb_{17}O_8Cl_{18}$: a promising IR nonlinear optical material with large laser damage threshold synthesized in an open system, J. Am. Chem. Soc. 137 (2015) 8360–8363.

[60] J. Yao, D. Mei, L. Bai, Z. Lin, W. Yin, P. Fu, Y. Wu, $BaGa_4Se_7$: a new congruent-melting IR nonlinear optical material, Inorg. Chem. 49 (2010) 9212–9216.

[61] X. Lin, G. Zhang, N. Ye, Growth and characterization of $BaGa_4S_7$: a new crystal for Mid-IR nonlinear optics, Cryst. Growth Des. 9 (2009) 1186–1189.

[62] J. Zhang, Z. Zhang, Y. Sun, C. Zhang, S. Zhang, Y. Liu, X. Tao, $MgTeMoO_6$: a neutral layered material showing strong second-harmonic generation, J. Mater. Chem. 22 (2012) 9921.

[63] S.G. Zhao, X.X. Jiang, R. He, S.Q. Zhang, Z.H. Sun, J.H. Luo, Z.S. Lin, M.C. Hong, A combination of multiple chromophores enhances second-harmonic generation in a nonpolar noncentrosymmetric oxide: $CdTeMoO_6$, J. Mater. Chem. C Mater. Opt. Electron. Devices 1 (2013) 2906–2912.

[64] S.G. Zhao, J.H. Luo, P. Zhou, S.Q. Zhang, Z.H. Sun, M.C. Hong, $ZnTeMoO_6$: a strong second-harmonic generation material originating from three types of asymmetric building units, RSC Adv. 3 (2013) 14000–14006.

[65] C. Jin, M. Wan, L. Huang, J. Shao, F. Wang, Experimental and theoretical studies of optical and nonlinear optical properties for $MnTeMoO_6$ crystal, J. Alloys. Compd. 651 (2015) 585–589.

[66] Q.T. Gu, C.S. Fang, W. Shi, X.W. Wu, Q.W. Pan, New wide-band nonlinear optics $CsGeCl_3$ crystal, J. Cryst. Growth 225 (2001) 501–504.

[67] L.C. Tang, J.Y. Huang, C.S. Chang, M.H. Lee, L.Q. Liu, New infrared nonlinear optical crystal $CsGeBr_3$: synthesis, structure and powder second-harmonic generation properties, J. Phys. Condens. Matter 17 (2005) 7275–7286.

[68] Z.-G. Lin, L.-C. Tang, C.-P. Chou, Characterization and properties of infrared NLO crystals: $AGeX_3$ (A = Rb, Cs; X = Cl, Br), J. Cryst. Growth 310 (2008) 3224–3229.

[69] Z.-G. Lin, L.-C. Tang, C.-P. Chou, Characterization and properties of novel infrared nonlinear optical crystal $CsGe(Br_xCl_{1-x})_3$, Inorg. Chem. 47 (2008) 2362–2367.

[70] G. Walters, E.H. Sargent, Electro-optic response in germanium halide perovskites, J. Phys. Chem. Lett. 9 (2018) 1018–1027.

[71] Z.-G. Lin, L.-C. Tang, C.-P. Chou, Study on Mid-IR NLO crystals $CsGe(Br_xCl_{1-X})_3$, Opt. Mater. (Amst) 31 (2008) 28–34.

[72] X.M. Jiang, S.P. Guo, H.Y. Zeng, M.J. Zhang, G.C. Guo, Large crystal growth and new crystal exploration of mid-infrared second-order nonlinear optical materials, Struct Bond 145 (2012) 1–43.

[73] S.-P. Guo, Y. Chi, G.-C. Guo, Recent achievements on middle and far-infrared second-order nonlinear optical materials, Coord. Chem. Rev. 335 (2017) 44–57.

[74] F. Liang, L. Kang, Z. Lin, Y. Wu, Mid-infrared nonlinear optical materials based on metal chalcogenides: structure–property relationship, Cryst. Growth Des. 17 (2017) 2254–2289.

[75] F. Liang, L. Kang, Z. Lin, Y. Wu, C. Chen, Analysis and prediction of Mid-IR nonlinear optical metal sulfides with diamond-like structures, Coord. Chem. Rev. 333 (2017) 57–70.

[76] I. Chung, M.G. Kanatzidis, Metal chalcogenides: a rich source of nonlinear optical materials, Chem. Mater. (2013) 130809094452006.

[77] L.-C. Tang, Y.-C. Chang, J.-Y. Huang, M.-H. Lee, C.-S. Chang, First principles calculations of linear and second-order optical responses in rhombohedrally distorted perovskite ternary halides, $CsGeX_3$(X = Cl, Br, and I), J. Appl. Phys. 48 (2009) 112402.

[78] L. Kang, D.M. Ramo, Z. Lin, P.D. Bristowe, J. Qin, C. Chen, First principles selection and design of Mid-IR nonlinear optical halide crystals, J. Mater. Chem. C

Mater. Opt. Electron. Devices 1 (2013) 7363–7370.

[79] Q. Zhang, Q. Jing, H. Duan, H. Cao, The relationship between covalent bonds and the optical response in a nonpolar family ATeMoO$_6$ (A = Mg, Zn, Cd): a berry-phase investigation, J. Solid State Chem. 264 (2018) 22–28.

[80] H. Mushahali, B. Mu, Q. Wang, M. Mamat, H. Cao, G. Yang, Q. Jing, A strategy for optical properties investigation in ABe$_2$BO$_3$F$_2$ (A = K, Rb, Cs) using finite field methods, Physica B Condens. Matter 541 (2018) 111–115.

[81] Q. Jing, G. Yang, Z. Chen, X. Dong, Y. Shi, A joint strategy to evaluate the microscopic origin of the second-harmonic-Generation response in nonpolar ABCO$_3$F compounds, Inorg. Chem. 57 (2018) 1251–1258.

[82] Z. Li, Q. Liu, Y. Wang, T. Iitaka, H. Su, T. Tohyama, Z. Yang, S. Pan, Second-harmonic generation in Noncentrosymmetric Phosphates, Phys. Rev. B 96 (2017) 035205.

[83] Z. Li, et al., Nonlinear electronic polarization and optical response in borophosphate BPO$_4$, Phys. Rev. B 93 (2016) 245125.

[84] X. Gonze, et al., Abinit: first-principles approach to material and nanosystem properties, Comput. Phys. Commun. 180 (2009) 2582–2615.

[85] X. Gonze, A brief introduction to the abinit software package, Z. Fã¼r Krist. - Cryst. Mater. (2005) 220.

[86] X. Gonze, et al., First-principles computation of material properties: the abinit software project, Comp. Mater. Sci. 25 (2002) 478–492.

[87] D.R. Hamann, Optimized Norm-Conserving vanderbilt pseudopotentials, Phys. Rev. B 88 (2013) 085117.

[88] M. Veithen, X. Gonze, P. Ghosez, Nonlinear optical susceptibilities, raman efficiencies, and electro-optic tensors from first-principles density functional perturbation theory, Phys. Rev. B 71 (2005) 125107.

[89] S.J. Clark, M.D. Segall, C.J. Pickard, P.J. Hasnip, M.J. Probert, K. Refson, M.C. Payne, First principles methods using castep, Z. Kristallogr. 220 (2005) 567–570.

[90] J. Perdew, K. Burke, M. Ernzerhof, Generalized gradient approximation made simple, Phys. Rev. Lett. 77 (1996) 3865–3868.

[91] A. Rappe, K. Rabe, E. Kaxiras, J. Joannopoulos, Optimized pseudopotentials, Phys. Rev. B 41 (1990) 1227–1230.

[92] J.S. Lin, A. Qteish, M.C. Payne, V. Heine, Optimized and transferable nonlocal separable ab initio pseudopotentials, Phys. Rev. B 47 (1993) 4174–4180.

[93] J. Lin, M.-H. Lee, Z.-P. Liu, C. Chen, C. Pickard, Mechanism for linear and nonlinear optical effects in B-BaB$_2$O$_4$ crystals, Phys. Rev. B 60 (1999) 13380–13389.

[94] B. Zhang, M.-H. Lee, Z. Yang, Q. Jing, S. Pan, M. Zhang, H. Wu, X. Su, C.-S. Li, Simulated pressure-induced blue-shift of Phase-Matching region and nonlinear optical mechanism for K$_3$B$_6$O$_{10}$X (X = Cl, Br), Appl. Phys. Lett. 106 (2015) 031906.

[95] F. Tran, P. Blaha, Accurate band gaps of semiconductors and insulators with a semilocal exchange-correlation potential, Phys. Rev. Lett. 102 (2009) 226401.

[96] J.P. Perdew, M. Levy, Physical content of the exact kohn-sham orbital energies: band gaps and derivative discontinuities, Phys. Rev. Lett. 51 (1983) 1884–1887.

[97] Z. Chen, Z. Zhang, R. Wu, X. Dong, Y. Shi, Q. Jing, Theoretical study on Pb$_2$VO$_2$F$_5$: large birefringence derived from optical anisotropies of VO$_2$F$_4$ groups, J. Mater. Sci. 53 (2017) 3483–3492.

[98] F. Zhang, F. Zhang, Q. Jing, S. Pan, Z. Yang, D. Jia, Synthesis, Crystal Structure and Properties of the Strontium Vanadate Fluoride Sr$_5$(VO$_4$)$_3$F, Z. Anorg. Allg. Chem. 641 (2015) 1211–1215.

[99] L. Li, Q. Jing, Z. Yang, X. Su, B.-H. Lei, S. Pan, F. Zhang, J. Zhang, Effect of the tetrahedral groups on the optical properties of LaBRO$_5$ (R = Si and Ge): a first-principles study, J. Appl. Phys. 118 (2015) 113104.

[100] Q. Jing, Z. Yang, S. Pan, D. Xue, Contribution of Lone-Pairs to birefringence affected by the Pb(II) coordination environment: a DFT investigation, Phys. Chem. Chem. Phys. 17 (2015) 21968–21973.

[101] Q. Jing, X. Dong, X. Chen, Z. Yang, S. Pan, C. Lei, The lone-pairs enhanced birefringence and SHG response: a DFT investigation on M$_2$B$_5$O$_9$Cl (M = Sr, Ba, and Pb), Chem. Phys. 453-454 (2015) 42–46.

[102] S. Han, Y. Wang, Q. Jing, H. Wu, S. Pan, Z. Yang, Effect of the cation size on the framework structures of magnesium tungstate, A$_4$Mg(WO$_4$)$_3$ (A = Na, K), R$_2$Mg$_2$(WO$_4$)$_3$ (R = Rb, Cs), Dalton Trans. 44 (2015) 5810–5817.

[103] B. Zhang, Z. Yang, Y. Yang, M.-H. Lee, S. Pan, Q. Jing, X. Su, P–(P,π*) interaction mechanism revealing and accordingly designed new member in Deep-Ultraviolet NLO borates Li$_n$M$_{n-1}$B$_{2n-1}$O$_{4n-2}$ (M = Cs/Rb, N = 3, 4, 6), J. Mater. Chem. C Mater. Opt. Electron. Devices 2 (2014) 4133–4141.

[104] A. Walsh, G.W. Watson, The origin of the stereochemically active Pb(II) lone pair: DFT calculations on PbO and PbS, J. Solid State Chem. 178 (2005) 1422–1428.

[105] D.J. Payne, R.G. Egdell, A. Walsh, G.W. Watson, J. Guo, P.A. Glans, T. Learmonth, K.E. Smith, Electronic origins of structural distortions in post-transition metal oxides: experimental and theoretical evidence for a revision of the lone pair model, Phys. Rev. Lett. 96 (2006) 157403.

[106] A. Walsh, D.J. Payne, R.G. Egdell, G.W. Watson, Stereochemistry of post-transition metal oxides: revision of the classical lone pair model, Chem. Soc. Rev. 40 (2011) 4455–4463.

[107] N.A. Spaldin, A beginner's guide to the modern theory of polarization, J. Solid State Chem. 195 (2012) 2–10.

[108] Q. Jing, X. Dong, Z. Yang, S. Pan, B. Zhang, X. Huang, M. Chen, The interaction between cations and anionic groups inducing SHG enhancement in a series of apatite-like crystals: a first-principles study, J. Solid State Chem. 219 (2014) 138–142.